Perampanel inhibits α-synuclein transmission in Parkinson's disease models

Jun Ueda, M.D.[1], Norihito Uemura, M.D., Ph.D.[1*], Masanori Sawamura, M.D.[1], Tomoyuki Taguchi, M.D.[1], Masashi Ikuno, M.D., Ph.D.[1], Seiji Kaji, M.D., Ph.D.[1], Yosuke Taruno, M.D.[1], Shuichi Matsuzawa, Ph.D.[1], Hodaka Yamakado, M.D., Ph.D.[1], Ryosuke Takahashi, M.D., Ph.D.[1*]

[1]Department of Neurology, Kyoto University Graduate School of Medicine

54 Shogoin, Kawaramachi, Sakyo-ku, Kyoto 606-8507 Japan

*Correspondence to:

Norihito Uemura, M.D., Ph.D. and Ryosuke Takahashi, M.D., Ph.D.

Department of Neurology, Kyoto University Graduate School of Medicine

54 Shogoin, Kawaramachi, Sakyo-ku, Kyoto 606-8507 Japan

Tel.: +81-75-751-4397

Fax: +81-75-761-9780

E-mail: nuemura@kuhp.kyoto-u.ac.jp (NU), ryosuket@kuhp.kyoto-u.ac.jp (RT)

ORCID ID: 0000-0002-6251-0810 (NU), 0000-0002-1407-9640 (RT)

Word Count: 3,672 words

Running title: Perampanel inhibits α-synuclein transmission

Keywords: Parkinson's disease, alpha-synuclein, neuronal activity, perampanel, macropinocytosis

Relevant conflicts of interests/financial disclosures: Nothing to report.

Funding Sources: This study was supported by a grant from the Ministry of Education, Culture, Sports, Science, and Technology (No. 19K16610, RT, Grant-in-Aid for Scientific Research (A); No. JP18H04041, Grant-in-Aid for Scientific Research on Innovative Areas; No. JP17H05698), the Integrated Neurotechnologies for Disease Studies (Brain/MINDS) from Japan Agency for Medical Research and Development AMED (RT, No. JP18dm0207020 and JP19dm0207070).

Abstract

Background: The intercellular transmission of pathogenic proteins plays a key role in the clinicopathological progression of neurodegenerative diseases. Previous studies have demonstrated that this uptake and release process is regulated by neuronal activity.

Objective: To examine the effect of perampanel, an antiepileptic drug, on α-synuclein transmission in cultured cells and mouse models of Parkinson's disease.

Methods: Mouse primary hippocampal neurons were transduced with α-synuclein preformed fibrils to examine the effect of perampanel on the development of α-synuclein pathology and its mechanisms of action. An α-synuclein preformed fibrils-injected mouse model was used to validate the effect of oral administration of perampanel on the α-synuclein pathology *in vivo*.

Results: Perampanel inhibited the development of α-synuclein pathology in mouse hippocampal neurons transduced with α-synuclein preformed fibrils. Interestingly, perampanel blocked the neuronal uptake of α-synuclein preformed fibrils by inhibiting macropinocytosis in a neuronal activity-dependent manner. We confirmed that oral administration of perampanel ameliorated the development of α-synuclein pathology in wild-type mice inoculated with α-synuclein preformed fibrils.

Conclusion: Modulation of neuronal activity could be a promising therapeutic target for Parkinson's disease, and perampanel could be a novel disease-modifying drug for Parkinson's disease.

Introduction

Parkinson's disease (PD) is pathologically characterized by progressive neuronal degeneration and the presence of Lewy bodies, which are composed of misfolded α-synuclein (α-syn). There is currently no therapy that inhibits or even slows down the progression of PD. Based on postmortem analysis, Braak et al. proposed a pathological staging of PD, in which the Lewy pathology in PD starts from the olfactory bulb (OB), anterior olfactory nucleus (AON), and dorsal nucleus of the vagus nerve and then spreads stereotypically to other interconnected brain regions.[1] Accumulating evidence suggests that misfolded α-syn behaves in a prion-like fashion and plays a significant role in PD progression.[2–14] Moreover, other pathogenic proteins, such as amyloid-β (Aβ) and tau in Alzheimer's disease (AD), are also thought to propagate in the brain and contribute to disease progression.[15] Although previous studies have revealed that exogenous α-syn preformed fibrils (PFFs) induce the propagation of α-syn pathology in cultured neurons[9] and mouse brains,[4, 5, 16] the molecular mechanisms and modulating factors underlying the propagation of α-syn pathology remain poorly understood.

Interestingly, a recent study demonstrated that the extracellular α-syn levels and α-syn release are affected by neuronal activity.[17] Moreover, extracellular release of tau, the formation of Aβ plaque, and the propagation of tau in AD are also affected by neuronal

activity.[18–20] We hypothesized that the inhibition of neuronal activity could modulate the dynamics of α-syn, inhibit the propagation of α-syn pathology, and attenuate the progression of PD.

Perampanel (PER) is an α-amino-3-hydroxy-5-methyl-4-isoxazolepropionic acid (AMPA) receptor antagonist that inhibits neuronal activity by blocking the AMPA receptor-induced sodium and calcium influx into neurons.[21–23] PER has been shown to equipotently inhibit AMPA receptors in both glutamatergic and GABAergic neurons, and suppression of neuronal activity by PER has been demonstrated in previous *in vitro* and *ex vivo* studies.[21–26] In the present study, we examined whether the inhibition of neuronal activity by PER could attenuate the propagation of α-syn pathology.

Materials and Methods

Animals

C57BL/6J 3-month-old male mice (n = 46) were obtained from Shimizu Laboratory Supplies Co., Ltd., or CLEA Japan, Inc. All breeding, housing, and experimental procedures were conducted according to the guidelines for animal care of Kyoto University and were approved by the Kyoto University Animal Care and Use Committee.

87

88 **Preparation of recombinant α-syn monomers and PFFs**

89 Mouse α-syn PFFs were generated as described previously.[27] We sonicated α-syn PFFs
90 for 10 min (30-s sonication followed by an interval of 30 s, for a total of 10 min) with a
91 Bioruptor bath sonicator before the administration of α-syn PFFs.

92

93 **Stereotaxic injection**

94 Stereotaxic injection was performed as previously described.[28, 29] The 3-month-old male
95 mice anesthetized with Avertin (1.875% [w/v] 2,2,2-tribromoethanol, 1.25% [v/v] 3-methyl-
96 1-butanol) were stereotaxically injected with 0.5 μL of α-syn PFFs (5 mg/mL) bilaterally
97 into the OB (coordinates: AP: +4.5 mm, L or R: −0.9 mm, DV: −1.5 mm relative to the
98 bregma and scull surface) using a 33-gauge microsyringe.

99

100 **PER treatment**

101 PER powder (Eisai Co., Ltd.) was suspended in a 0.5% (w/v) methyl cellulose solution
102 (final concentration of PER: 2.0 mg/mL, Wako), and 10 μL/g of body weight was orally
103 administered to the mice daily. The 3-month-old male mice were initially treated with 20

mg/kg PER before injection of α-syn PFFs (PER [pre], n = 8), 20 mg/kg PER after injection of α-syn PFFs (PER [post], n = 6), or vehicle before injection of α-syn PFFs (control, n = 7). The dose of PER was determined according to previous reports.[30, 31] Treatment with PER or vehicle was continued for 2 weeks after injection of α-syn PFFs.

Immunohistochemistry

Immunohistochemistry was performed as previously described, with minor modifications.[27, 28] Briefly, mice were sacrificed 2 weeks after injection of α-syn PFFs. The brains were fixed with 4% paraformaldehyde (PFA), embedded in paraffin, and processed to prepare 8-μm sections. An antibody against phosphorylated-α-syn (p-α-syn; 1:5000; ab51253, Abcam) was used as the primary antibody. The areas of p-α-syn-positive pathology in the AON and piriform cortex (PC) were quantified using the ImageJ software. For the assessment of AON, the total p-α-syn-positive areas and total numbers of neuronal p-α-syn-positive aggregates were evaluated in the images of three coronal sections at +3.08, +2.80, and +2.58 mm relative to the bregma. For the assessment of PC, the total p-α-syn-positive areas and total numbers of neuronal p-α-syn-positive aggregates were evaluated

in the images of four coronal sections at +1.78, +0.38, −0.94, and −2.30 mm relative to the bregma.

Sequential extraction

Sequential extraction of brain lysates was performed as previously described.[32] For biochemical analysis, we dissected the ventral half of the cerebral cortex containing the AON and PC from phosphate buffered saline (PBS)-perfused brains of mice treated with 20 mg/kg PER or vehicle for 2 weeks without α-syn PFFs inoculation (n = 5, respectively; Fig. 4A, B) or mice treated with 20 mg/kg PER or vehicle for 2 weeks after injection of α-syn PFFs into the OB (n = 5, respectively; Fig. 4G).

Western blotting

Western blotting was performed as previously described, with minor modification.[33] Briefly, 10 μg of Triton X-soluble or Triton X-insoluble samples was dissolved in sample buffer (1% [w/v] sodium dodecyl sulfate [SDS], 12.5% [w/v] glycerol, 0.005% [w/v] bromophenol blue, 2.5% [w/v] 2-mercaptoethanol, 25 mM Tris-HCl, pH 6.8) and separated on 10%–20% (w/v) gradient gels (FUJIFILM Wako Pure Chemical Corporation). The proteins were transferred to polyvinylidene difluoride membranes (Merck Millipore). The membranes were treated with 4% (w/v) PFA in PBS for 30 min at room temperature (RT) before blocking to prevent detachment of α-syn from the blotted membranes. After blocking for 1 h with 5% [w/v] skim

milk in TBS-T, the membranes were incubated with primary antibodies against α-syn (1:2000; 610787, BD Biosciences), β-actin (1:5000; A5441, Sigma-Aldrich), and p-α-syn (1:5000; ab51253, Abcam) overnight at 4°C. Subsequently, the membranes were incubated with horseradish peroxidase-conjugated secondary antibodies (NB7574 or NB7160; Novus Biologicals) for 1 h at RT. Immunoreactive bands were detected using detection reagent (Thermo Fisher Scientific), and the chemiluminescent signal was detected with Amersham Imager 600 (GE Healthcare). The band intensities were normalized to those of β-actin.

Primary hippocampal culture

Primary hippocampal cell cultures were prepared from E16 ICR mice. The embryos were removed and decapitated, and the entire hippocampus was dissected under sterile conditions. After enzymatic digestion for 5 min by 0.25% trypsin at 37°C, the cells were separated by trituration in Dulbecco's modified Eagle's medium (Wako) supplemented with 10% fetal bovine serum (Thermo Fisher Scientific) and 1% penicillin–streptomycin (Thermo Fisher Scientific). After trituration, the solution was centrifuged at 190 g for 3 min, and the cell pellet was immediately re-suspended in Neurobasal medium (Thermo Fisher

157 Scientific) with 2% B27 (Invitrogen), 2 mM L-glutamine (Nacalai Tesque), and 1%
158 penicillin–streptomycin (Thermo Fisher Scientific). The dissociated cells were plated on
159 24-well plates (1.5×10^5 cells/well) that were pre-coated with poly-DL-ornithine
160 hydrobromide (Sigma-Aldrich). Half of the medium was removed and replaced every 3–4
161 days. The cells were cultured under constant conditions of 37°C, 5% CO_2 in a humidified
162 incubator. The experiments were conducted over 14–17 days *in vitro* (DIV), and each
163 experiment was repeated three times.
164
165 **Cytotoxicity with media LDH assay**
166 Cytotoxicity was assessed using media lactate dehydrogenase (LDH) Assay Kit
167 (Cytotoxicity LDH Assay Kit-WST, Dojindo). Supernatants (100 µL) was incubated with an
168 equal volume of assay buffer for 30 min, and the absorbance of the culture medium was
169 measured using a microplate reader at a test wavelength of 490 nm.
170
171 **α-syn PFFs, pHrodo-PFFs, and pHrodo-dextran transduction**
172 Sonicated α-syn PFFs were labeled with pHrodo Red (Invitrogen), as per the
173 manufacturer's instruction. α-syn PFFs (final concentration: 0.05 µg/mL), α-syn PFFs

174 labeled with pHrodo Red (pHrodo-PFFs; final concentration: 0.5 μg/mL), and pHrodo Red-
175 dextran (10 kDa; Invitrogen), (pHrodo-dextran; final concentration: 0.5 μg/mL) were added
176 to the primary hippocampal culture at 14 DIV with PER (0.3, 3, 10, or 30 μM), 2,3-Dioxo-6-
177 nitro-1,2,3,4-tetrahydrobenzo[*f*]quinoxaline-7-sulfonamide (NBQX; 50 μM, Abcam),
178 tetrodotoxin (TTX; 1 μM, Nacalai Tesque), 5-(N-ethyl-N-isopropyl)-amiloride (EIPA; 50 μM,
179 Cayman Chemical), or vehicle and then incubated for the indicated time. The dose of PER
180 was determined according to previous reports.[21, 23] Primary neurons transduced with PBS
181 alone were used as negative controls.
182
183 **Immunocytochemistry**
184 For immunocytochemistry, the cells were washed twice with PBS and then fixed with 4%
185 (w/v) PFA in PBS for 5–20 min. After washing twice with PBS, incubation with
186 PBS/0.1%Tween (10 min), and blocking with 3% (w/v) bovine serum albumin/PBS (1 h at
187 RT), the cells were incubated with primary antibodies against p-α-syn (1:3000; ab51253,
188 Abcam), glial fibrillary acidic protein (GFAP; 1:500; M1406, Sigma-Aldrich), and neuronal
189 nuclei (NeuN; 1:500; ABN78, Merck Millipore) at 4°C overnight. After washing with PBS,
190 the cells were incubated with Alexa Fluor 488-conjugated (1:1000; A11001, Invitrogen),

191 594-conjugated (1:1000; A11037, Invitrogen), or 647-conjugated secondary antibodies
192 (1:1000; A21094, Life Technologies) for 1 h at RT. After washing with PBS and cover-
193 slipping, the cells were observed with BZ-X710 (Keyence) at × 20 magnification. The
194 image acquisition settings were kept constant in all groups for each experiment. The
195 number of NeuN-positive cells per field were counted to measure neuronal density. The
196 areas of p-α-syn-positive pathology, pHrodo-PFFs, and pHrodo-dextran were quantified
197 using ImageJ software. The average areas of p-α-syn-positive pathology, pHrodo-PFFs,
198 and pHrodo-dextran per field (3–10 fields of view per sample) were averaged for the same
199 conditions.
200
201 **Statistical analysis**
202 Statistical analysis was conducted using PRISM statistical package. Statistical significance
203 was evaluated by employing Kruskal-Wallis test, followed by Dunn's *post hoc* test. Mann
204 Whitney test was employed to compare the two groups of data. Statistical significance was
205 set at $*P < 0.05$, $**P < 0.01$, or $***P < 0.001$.
206
207 **Results**

208

209 **PER inhibits the development of p-α-syn-positive pathology in hippocampal primary**

210 **neurons**

211 To investigate the potential effect of PER on PD pathology, we first assessed whether

212 PER is effective against the development of p-α-syn-positive pathology using an *in vitro*

213 PD model. In contrast to physiological α-syn, the majority of α-syn in Lewy pathology is

214 phosphorylated at Ser129; thus, p-α-syn is a useful pathological marker of human PD and

215 PD models.[4, 5, 10, 34] Primary neurons transduced with α-syn PFFs exhibit p-α-syn-positive

216 pathology and are well established as *in vitro* PD models to examine the mechanisms of

217 the prion-like propagation of α-syn pathology.[9] In this study, mouse hippocampal primary

218 neurons were transduced with α-syn PFFs in the presence of PER (0.3, 3, 10, or 30 μM) or

219 vehicle at 14 DIV, followed by immunocytochemistry at 17 DIV. Primary neurons

220 transduced with PBS alone were used as negative controls. To exclude the cytotoxic effect

221 of PER, we measured the neuronal density by counting the NeuN-positive cells, which

222 revealed no significant difference among the groups (Fig. 1A). Next, we tested the effect of

223 PER on the development of p-α-syn-positive pathology. Interestingly,

224 immunocytochemistry revealed that less p-α-syn-positive pathology was observed in

primary neurons transduced with α-syn PFFs in the presence of PER compared with those without PER (Fig. 1B, C). Primary neurons transduced with PBS alone exhibited no p-α-syn-positive pathology (Fig. 1C).

PER inhibits the activity-dependent uptake of α-syn PFFs via macropinocytosis in hippocampal primary neurons

To elucidate the mechanisms of the decreased p-α-syn-positive pathology in α-syn PFFs-transduced primary neurons treated with PER, we investigated the potential effect of PER against the neuronal uptake of α-syn PFFs. We generated pHrodo-PFFs to examine the effect of PER on the uptake of α-syn PFFs in primary hippocampal neurons. Due to its favorable pH-sensitive photophysical properties, pHrodo Red is widely used for studying endocytosis.[35, 36] In this study, at 14 DIV, primary hippocampal neurons were transduced with pHrodo-PFFs in the presence of PER (0.3, 3, 10, or 30 μM) or vehicle, incubated for 4 h, followed by LDH assay, evaluation of the areas of pHrodo-PFFs, and immunocytochemistry. Primary neurons transduced with PBS alone were used as negative controls. The neuronal density was measured to exclude cytotoxic effects of PER, and no significant difference was found among the groups (Fig. 2A). Moreover, LDH release into

242 the conditioned medium did not differ among the groups (Fig. 2B), suggesting that PER
243 treatment exhibited no appreciable toxicity to primary neurons within the 4-h incubation
244 period. Next, we assessed whether pHrodo-PFFs colocalize with NeuN, a neuronal
245 marker, or GFAP, an astrocytic marker. Immunocytochemical analyses revealed only a
246 small number of GFAP-positive cells and those cells colocalized with pHrodo-PFFs
247 compared to NeuN-positive cells (Fig. 2C, Supporting Information Fig. S1A, B). It has been
248 reported that both astrocytes and neurons efficiently take up α-syn PFFs. [37] However,
249 because the number of astrocytes was considerably lower than that of neurons in our
250 primary neuronal culture (Fig. 2C, Supporting Information Fig. S1A, B), the fluorescence of
251 pHrodo-PFFs was mostly observed in neurons. Therefore, the fluorescence of pHrodo-
252 PFFs observed in this study can be considered as neuronal uptake of α-syn PFFs. We
253 next tested the effect of PER on the neuronal uptake of α-syn PFFs. PER treatment
254 decreased the pHrodo-PFFs areas compared to the control in a dose-dependent manner,
255 indicating a reduction in the uptake of α-syn PFFs by these neurons (Fig. 2D, G), while
256 primary neurons transduced with PBS alone exhibited no fluorescence (Fig. 2G). To
257 confirm the mechanisms of action of PER, we tested the effect of NBQX, another AMPA
258 receptor antagonist, and TTX, a sodium channel blocker, on the neuronal uptake of α-syn

PFFs. Both NBQX (50 μM) and TTX (1 μM) treatment decreased the pHrodo-PFFs areas without toxicity (Fig. 2E, F, Supporting Information Fig. S2A–D).

Although the mechanisms of α-syn PFFs uptake are not fully understood, several previous studies have demonstrated that α-syn PFFs uptake could be mediated by the endocytic process, including macropinocytosis.[36, 38] Therefore, we investigated the effect of PER on macropinocytosis. First, we investigated whether macropinocytosis is involved in the neuronal α-syn PFFs uptake in the hippocampal primary neurons. EIPA is a specific inhibitor of macropinocytosis that blocks the Na^+/H^+ exchanger without affecting other endocytic pathways, such as clathrin-mediated endocytosis.[39–42] Hippocampal primary neurons transduced with pHrodo-PFFs in the presence of EIPA exhibited a remarkable decrease in pHrodo-PFFs areas without decreasing neuronal density (Fig. 3A–C). Next, we tested the efficacy of PER against macropinocytosis. Dextran (10 kDa) is a marker of fluid phase endocytosis; it is widely used to quantify macropinocytosis.[38–40] In this study, the hippocampal primary neurons were treated with pHrodo-dextran in the presence of PER (0.3, 3, 10, or 30 μM), NBQX (50 μM), TTX (1 μM), or vehicle at 14 DIV and then incubated for 4 h. PER, NBQX, and TTX treatment resulted in decreased areas of pHrodo-

dextran, indicating the inhibition of macropinocytosis in hippocampal primary neurons (Fig. 3D–G).

PER inhibits the development of p-α-syn-positive pathology in a mouse PD model

We further investigated the effect of PER on the propagation of α-syn pathology in a mouse PD model. First, we checked the expression levels of α-syn and p-α-syn in mouse brains by Western blot analysis to exclude the possibility that they are affected by PER administration. To this end, wild type mice were treated orally with PER or vehicle for 2 weeks, and brain lysates containing AON and PC were sequentially extracted in Triton X and SDS buffers, followed by Western blotting. Western blot analysis revealed that PER had no significant effect on the expression levels of total α-syn and p-α-syn in the Triton X-soluble fraction (Fig. 4A, B).

Next, we examined whether PER treatment is also effective in an *in vivo* PD model. We previously reported that mice inoculated with α-syn PFFs into the OB, one of the initial lesions in PD, exhibited α-syn pathology mainly in the olfactory pathway, including the AON and PC, at 1 month post-inoculation, but not in mice inoculated with PBS. [28] In this study, we analyzed wild type mice inoculated with α-syn PFFs into the OB

292 bilaterally by stereotaxic injections with or without oral administration of PER. PER
293 treatment was initiated before or after the injection of α-syn PFFs, and mice were
294 sacrificed 2 weeks after injection (Fig. 4C). In this study, “PER (pre)” refers to “the mice in
295 which PER treatment was initiated before the injection of α-syn PFFs,” whereas “PER
296 (post)” refers to “the mice in which PER treatment was initiated after the injection of α-syn
297 PFFs.” Mice in which the treatment was started with vehicle alone before the injection of α-
298 syn PFFs were used as a control group (Fig. 4C). We analyzed the areas of p-α-syn-
299 positive pathology and the number of neuronal p-α-syn-positive aggregates in the AON
300 and PC, as described previously.[28] In PER (pre), the areas of p-α-syn-positive pathology in
301 the AON and PC were significantly decreased compared with those in the control (Fig. 4D,
302 E); in PER (post), they were not significantly decreased compared with those in the
303 control, although there was a tendency toward decreased p-α-syn-positive pathology (Fig.
304 4D, E). Moreover, the numbers of neuronal p-α-syn-positive aggregates in the AON and
305 PC were also significantly decreased in PER (pre), but not in PER (post) (Fig. 4F). We
306 also investigated the amount of p-α-syn-positive aggregates by Western blot analysis. A
307 previous study reported p-α-syn-positive bands in the detergent-insoluble fraction of
308 mouse brains inoculated with α-syn PFFs by Western blot analysis.[5] In the current study,

309 brain lysates containing the AON and PC of PER (pre), PER (post), or control were
310 sequentially extracted in Triton X and SDS buffers, followed by Western blotting. In
311 accordance with the immunohistochemical results, Western blot analysis showed
312 significantly decreased p-α-syn in the Triton X-insoluble fraction of PER (pre) and PER
313 (post) compared to that in the control (Fig. 4G).
314

315 **Discussion**

316 Although numerous studies have reported on the propagation of α-syn pathology in
317 cultured neurons and mice, the correlation between the neuronal activity and the
318 propagation of α-syn pathology remains unclear. Here we used *in vitro* and *in vivo* PD
319 models to demonstrate that neuronal activity plays a crucial role in the propagation of α-
320 syn pathology. We found that PER, as well as NBQX and TTX inhibit the neuronal uptake
321 of α-syn PFFs and decrease the development of p-α-syn-positive pathology in primary
322 neurons. PER and NBQX inhibit neuronal activity by blocking the AMPA receptor
323 current,[23, 43] whereas TTX suppresses neuronal activity in an AMPA receptor-independent
324 manner by blocking the voltage-gated sodium channel. Thus, our results strongly suggest
325 that the neuronal uptake of α-syn PFFs is mediated by an activity-dependent mechanism,

and PER inhibits the formation of p-α-syn-positive pathology by reducing the activity-dependent neuronal uptake of α-syn PFFs. Another important finding is that the inhibitor of macropinocytosis remarkably decreased α-syn PFFs uptake, and PER, NBQX, and TTX inhibited macropinocytosis in primary neurons. Macropinocytosis is a type of fluid phase endocytosis that is characterized by the formation of large endocytic vesicles termed macropinosomes (up to 5 μm). Previously, we demonstrated that the length of sonicated α-syn PFFs was 66.8 ± 3.1 nm (mean ± standard error of the mean [SEM]),[44] which suggests that a macropinosome is large enough for α-syn PFFs uptake. Although several studies have revealed that macropinocytosis could be involved in the uptake of pathogenic proteins in neurodegenerative diseases,[38–40] the correlation between macropinocytosis and neuronal activity has not yet been reported. Our results demonstrate that neuronal macropinocytosis is involved in the uptake of α-syn PFFs and is regulated, at least in part, by neuronal activity. Taken together, our *in vitro* results suggest that PER inhibits neuronal α-syn PFFs uptake by suppressing macropinocytosis in a neuronal activity-dependent manner.

Our *in vivo* results suggest that PER inhibits the development of p-α-syn pathology induced by α-syn PFFs without affecting the levels of total α-syn and p-α-syn

343 expression, which is consistent with our *in vitro* results. Furthermore, our *in vivo* results
344 also suggest that the presence or absence of PER treatment at the time of α-syn PFFs
345 injection affects the development of p-α-syn-positive pathology (Fig. 4D–G). Since the
346 neuronal uptake of α-syn PFFs is the initial step of propagation, and starts immediately
347 after α-syn PFFs injection,[45] the neuronal uptake of α-syn PFFs in PER (pre) could be
348 more reduced than that in PER (post), leading to further reduction of p-α-syn-positive
349 pathology in PER (pre). These results are consistent with the rapid transmission of α-syn
350 PFFs via synaptic connections that was previously observed in a mouse PD model.[46] In
351 this study, we assessed the neuronal uptake of α-syn PFFs and the initial development of
352 α-syn pathology. However, since our *in vivo* PD model showed neuronal death more than
353 3 months after the injection of α-syn PFFs,[28] the duration of our *in vivo* study was
354 insufficient to evaluate the long-term efficacy of PER. Further *in vivo* studies with longer
355 follow-up are required to elucidate any negative effects of PER as well as to determine the
356 long-term effect of PER on the subsequent propagation of α-syn pathology, neuronal
357 death, and behavioral changes in PD models. Moreover, several clinical studies have
358 reported that PER treatment has no beneficial effect on clinical symptoms in PD
359 patients.[47, 48] However, since the aim of these clinical studies was to evaluate the efficacy

of PER against wearing off, the patients with PD were at an advanced stage and the duration of PER treatment was relatively short (≤ 30 weeks). In order to elucidate the disease-modifying effect of PER, *de novo* patients with PD should be treated with PER for a longer duration (e.g., 36 months). After further validation of the effects of PER in animal studies, such clinical studies should be considered.

In conclusion, the major finding of this study is that PER inhibits the activity-dependent neuronal uptake of α-syn PFFs via macropinocytosis, and the subsequent development of p-α-syn-positive pathology in PD models. Our results support the idea that the propagation of α-syn pathology could be affected by an activity-dependent mechanism in neurons and suggest that PER could inhibit the neuronal transmission of pathogenic α-syn, thus slowing the progression of PD. Considering that neurodegenerative diseases have similar mechanisms of pathogenic protein transmission, PER could also be applied to other neurodegenerative diseases. Furthermore, since PER has already been approved as an antiepileptic drug in many countries, prompt clinical application for PD and other neurodegenerative diseases is possible. Targeting neuronal activity with PER could represent a new therapeutic strategy for synucleinopathies including PD and other neurodegenerative diseases.

Acknowledgments

We wish to thank Yusuke Hatanaka Ph.D., Ms. Rie Hikawa and Ms. Ikuko Amano for the technical assistance, and Eisai Co., Ltd. for providing us with PER.

Author contributions

JU, MS, NU, and HY designed the experiments. JU performed the experiments. JU and NU wrote the manuscript after a fruitful discussion with MS, TT, MI, SK, YT, SM, and HY. All the authors have read and approved the final manuscript. RT supervised all the experiments.

References

1. Braak H, Del Tredici K, Rüb U, de Vos RA, Jansen Steur EN, Braak E. Staging of brain pathology related to sporadic Parkinson's disease. Neurobiol Aging 2003; 24: 197-211.
2. Olanow CW, Prusiner SB. Is Parkinson's disease a prion disorder? Proc Natl Acad Sci 2009; 106: 12571-12572.
3. Lee SJ, Desplats P, Lee HJ, Spencer B, Masliah E. Cell-to-cell transmission of α-synuclein aggregates. Methods Mol Biol 2012; 849: 347-359.

4. Luk KC, Kehm V, Carroll J, et al. Pathological α-synuclein transmission initiates Parkinson-like neurodegeneration in nontransgenic mice. Science 2012; 338: 949-953.

5. Masuda-Suzukake M, Nonaka T, Hosokawa M, et al. Prion-like spreading of pathological α-synuclein in brain. Brain 2013; 136: 1128-1138.

6. Guo JL, Lee VM. Cell-to-cell transmission of pathogenic proteins in neurodegenerative diseases. Nat Med 2014; 20: 130-138.

7. Dehay B, Vila M, Bezard E, Brundin P, Kordower JH. Alpha-synuclein propagation: new insights from animal models. Mov Disord 2016; 31: 161-168.

8. Tyson T, Steiner JA, Brundin P. Sorting out release, uptake and processing of alpha-synuclein during prion-like spread of pathology. J Neurochem 2016; 139: 275-289.

9. Angot E, Brundin P. Dissecting the potential molecular mechanisms underlying alpha-synuclein cell-to-cell transfer in Parkinson's disease. Parkinsonism Relat Disord 2009; 15: S143-S147.

10. Volpicelli-Daley LA, Luk KC, Patel TP, et al. Exogenous α-synuclein fibrils induce Lewy body pathology leading to synaptic dysfunction and neuron death. Neuron 2011; 72: 57-71.

411 11. Freundt EC, Maynard N, Clancy EK, et al. Neuron-to-neuron transmission of α-
412 synuclein fibrils through axonal transport. Ann Neurol 2012; 72: 517-524.
413 12. Borchelt DR, Koliatsos VE, Guarnieri M, Pardo CA, Sisodia SS, Price DL. Rapid
414 anterograde axonal transport of the cellular prion glycoprotein in the peripheral and
415 central nervous systems. J Biol Chem 1994; 269: 14711-14714.
416 13. Cohen FE, Pan KM, Huang Z, Baldwin M, Fletterick RJ, Prusiner SB. Structural clues
417 to prion replication. Science 1994; 264: 530-531.
418 14. Moya KL, Hässig R, Créminon C, Laffont I, Di Giamberardino L. Enhanced detection
419 and retrograde axonal transport of PrPc in peripheral nerve. J Neurochem 2004; 88:
420 155-160.
421 15. Jucker M, Walker LC. Self-propagation of pathogenic protein aggregates in
422 neurodegenerative diseases. Nature 2013; 501: 45-51.
423 16. Rey NL, Steiner JA, Maroof N, et al. Widespread transneuronal propagation of α-
424 synucleinopathy triggered in olfactory bulb mimics prodromal Parkinson's disease. J
425 Exp Med 2016; 213: 1759-1778.

426 17. Yamada K, Iwatsubo T. Extracellular α-synuclein levels are regulated by neuronal
427 activity. Mol Neurodegener 2018; 13: 9.
428 18. Bero AW, Yan P, Roh JH, et al. Neuronal activity regulates the regional vulnerability to
429 amyloid-β deposition. Nat Neurosci 2011; 14: 750-756.
430 19. Wu JW, Hussaini SA, Bastille IM, et al. Neuronal activity enhances tau propagation and
431 tau pathology in vivo. Nat Neurosci 2016; 19: 1085-1092.
432 20. Holth JK, Fritschi SK, Wang C, et al. The sleep-wake cycle regulates brain interstitial
433 fluid tau in mice and CSF tau in humans. Science 2019; 363: 880-884.
434 21. Hanada T, Hashizume Y, Tokuhara N, et al. Perampanel: a novel, orally active,
435 noncompetitive AMPA-receptor antagonist that reduces seizure activity in rodent
436 models of epilepsy. Epilepsia 2011; 52: 1331-1340.
437 22. Ceolin L, Bortolotto ZA, Bannister N, et al. A novel anti-epileptic agent, perampanel,
438 selectively inhibits AMPA receptor-mediated synaptic transmission in the hippocampus.
439 Neurochem Int 2012; 61: 517-522.
440 23. Chen CY, Matt L, Hell JW, Rogawski MA. Perampanel inhibition of AMPA receptor
441 currents in cultured hippocampal neurons. PLOS ONE 2014; 9: e108021.

442 24. Fukushima K, Hatanaka K, Sagane K, Ido K. Inhibitory effect of anti-seizure
443 medications on ionotropic glutamate receptors: special focus on AMPA receptor
444 subunits. Epilepsy Res 2020; 167: 106452.

445 25. Barygin OI. Inhibition of calcium-permeable and calcium-impermeable AMPA receptors
446 by perampanel in rat brain neurons. Neurosci Lett 2016; 633: 146-151.

447 26. Yang YC, Wang GH, Chuang AY, Hsueh SW. Perampanel reduces paroxysmal
448 depolarizing shift and inhibitory synaptic input in excitatory neurons to inhibit epileptic
449 network oscillations. Br J Pharmacol 2020; 177: 5177-5194.

450 27. Uemura N, Yagi H, Uemura MT, Hatanaka Y, Yamakado H, Takahashi R. Inoculation
451 of α-synuclein preformed fibrils into the mouse gastrointestinal tract induces Lewy
452 body-like aggregates in the brainstem via the vagus nerve. Mol Neurodegener 2018;
453 13: 21.

454 28. Uemura N, Uemura MT, Lo A, et al. Slow progressive accumulation of oligodendroglial
455 alpha-synuclein (α-syn) pathology in synthetic α-syn fibril-induced mouse models of
456 synucleinopathy. J Neuropathol Exp Neurol 2019; 78: 877-890.

29. Uemura N, Ueda J, Yoshihara T, et al. α-Synuclein Spread from Olfactory Bulb Causes Hyposmia, Anxiety, and Memory Loss in BAC-SNCA Mice. Mov Disord 2021; Online ahead of print.

30. Akamatsu M, Yamashita T, Hirose N, Teramoto S, Kwak S. The AMPA receptor antagonist perampanel robustly rescues amyotrophic lateral sclerosis (ALS) pathology in sporadic ALS model mice. Sci Rep 2016; 6: 28649.

31. Sugiyama K, Aida T, Nomura M, Takayanagi R, Zeilhofer HU, Tanaka K. Calpain-dependent degradation of nucleoporins contributes to motor neuron death in a mouse model of chronic excitotoxicity. J Neurosci 2017; 37: 8830-8844.

32. Taguchi T, Ikuno M, Hondo M, et al. α-Synuclein BAC transgenic mice exhibit RBD-like behaviour and hyposmia: a prodromal Parkinson's disease model. Brain 2020; 143: 249-265.

33. Uemura N, Koike M, Ansai S, et al. Viable neuronopathic Gaucher disease model in Medaka (Oryzias latipes) displays axonal accumulation of alpha-synuclein. PLOS Genet 2015; 11: e1005065.

472 34. Fujiwara H, Hasegawa M, Dohmae N, et al. Alpha-synuclein is phosphorylated in
473 synucleinopathy lesions. Nat Cell Biol 2002; 4: 160-164.
474 35. Miksa M, Komura H, Wu R, Shah KG, Wang P. A novel method to determine the
475 engulfment of apoptotic cells by macrophages using pHrodo succinimidyl ester. J
476 Immunol Methods 2009; 342: 71-77.
477 36. Mao X, Ou MT, Karuppagounder SS, et al. Pathological α-synuclein transmission
478 initiated by binding lymphocyte-activation gene 3. Science 2016; 30: 353(6307).
479 37. Loria F, Vargas JY, Bousset L, et al. α-Synuclein transfer between neurons and
480 astrocytes indicates that astrocytes play a role in degradation rather than in spreading.
481 Acta Neuropathol 2017; 134: 789-808.
482 38. Holmes BB, DeVos SL, Kfoury N, et al. Heparan sulfate proteoglycans mediate
483 internalization and propagation of specific proteopathic seeds. Proc Natl Acad Sci
484 2013; 110: E3138-E3147.
485 39. Münch C, O'Brien J, Bertolotti A. Prion-like propagation of mutant superoxide
486 dismutase-1 misfolding in neuronal cells. Proc Natl Acad Sci 2011; 108: 3548-3553.

40. Zeineddine R, Pundavela JF, Corcoran L, et al. SOD1 protein aggregates stimulate macropinocytosis in neurons to facilitate their propagation. Mol Neurodegener 2015; 10: 57.

41. Gold S, Monaghan P, Mertens P, et al. A clathrin independent macropinocytosis-like entry mechanism used by bluetongue virus-1 during infection of BHK cells. PLOS ONE 2010; 5: e11360.

42. West MA, Bretscher MS, Watts C. Distinct endocytotic pathways in epidermal growth factor-stimulated human carcinoma A431 cells. J Cell Biol 1989; 109: 2731-2739.

43. Doyle MW, Andresen MC. Reliability of monosynaptic sensory transmission in brain stem neurons in vitro. J Neurophysiol 2001; 85: 2213-2223.

44. Uemura N, Yagi H, Uemura MT, Yamakado H, Takahashi R. Limited spread of pathology within the brainstem of α-synuclein BAC transgenic mice inoculated with preformed fibrils into the gastrointestinal tract. Neurosci Lett 2020; 716: 134651.

45. Rey NL, Petit GH, Bousset L, Melki R, Brundin P. Transfer of human α-synuclein from the olfactory bulb to interconnected brain regions in mice. Acta Neuropathol 2013; 126: 555-573.

503 46. Okuzumi A, Kurosawa M, Hatano T, et al. Rapid dissemination of alpha-synuclein
504 seeds through neural circuits in an in-vivo prion-like seeding experiment. Acta
505 Neuropathol Commun 2018; 6: 96.

506 47. Eggert K, Squillacote D, Barone P, et al. Safety and efficacy of perampanel in
507 advanced Parkinson's disease: a randomized, placebo-controlled study. Mov Disord
508 2010; 25: 896-905.

509 48. Lattanzi S, Grillo E, Brigo F, Silvestrini M. Efficacy and safety of perampanel in
510 Parkinson's disease. A systematic review with meta-analysis. J Neurol 2018; 265: 733-
511 740.

512

513 **FIGURE LEGENDS**

514

515 **FIG. 1**

516 PER inhibits the development of p-α-syn-positive pathology in primary hippocampal
517 neurons. (A) Density of neurons. In Fig. 1, "control" refers to the primary neurons that were
518 transduced with α-syn PFFs and treated with vehicle. Data are representative of three
519 independent experiments (n = 4–8). Data are normalized against control and are

expressed as mean ± SEM. N.S.: Not significant, Kruskal-Wallis test with Dunn's *post hoc* test. Scatter plots show data from each sample. (B) Area of p-α-syn-positive pathology in primary hippocampal neurons. Plotted data are representative of three independent experiments (n = 4–8). Data are normalized against control and are expressed as mean ± SEM. $^{**}P < 0.01$; Kruskal-Wallis test with Dunn's *post hoc* test. (C) Representative images of immunohistochemical staining of primary hippocampal neurons. Data are representative of three independent experiments. Arrows indicate p-α-syn colocalization with NeuN-positive cells. Scale bar: 20 μm.

FIG. 2

PER, NBQX, and TTX inhibit the uptake of α-syn PFFs in primary hippocampal neurons. (A) Density of neurons. In Fig. 2, "control" refers to the primary neurons that were transduced with pHrodo-PFFs and treated with vehicle. Data are representative of three independent experiments (n = 4–8). Data are normalized against control and are expressed as mean ± SEM. N.S.: Not significant, Kruskal-Wallis test with Dunn's *post hoc* test. Scatter plots show data from each sample. (B) LDH assay. Plotted data are representative of three independent experiments (n = 4–8). Data are normalized against

control and are expressed as mean ± SEM. N.S.: Not significant, Kruskal-Wallis test with Dunn's *post hoc* test. (C) Representative images of immunohistochemical staining of primary hippocampal neurons. Data are representative of three independent experiments. Arrows indicate pHrodo-PFFs colocalized with NeuN-positive cells, and arrowheads indicate GFAP-positive cells. Scale bar: 20 μm. (D) (E) (F) Area of pHrodo-PFFs in primary hippocampal neurons. Plotted data are representative of three independent experiments (n = 4–8). Data are normalized against control and are expressed as mean ± SEM. $^{**}P < 0.01$, $^{***}P < 0.001$, Kruskal-Wallis test with Dunn's *post hoc* test (D), and Mann Whitney test (E, F). (G) Representative images of pHrodo-PFFs in primary hippocampal neurons. Data are representative of three independent experiments. Scale bar: 20 μm.

FIG. 3

PER, NBQX, and TTX inhibit the uptake of α-syn PFFs via macropinocytosis. (A) Density of neurons. In Fig. 3A–3C, "control" refers to the primary neurons that were transduced with pHrodo-PFFs and treated with vehicle. Data are representative of three independent experiments (n = 6). Data are normalized against control and are expressed as mean ± SEM. N.S.: Not significant, Mann Whitney test. Scatter plots show data from each sample.

(B) Area of pHrodo-PFFs in primary hippocampal neurons. Plotted data are representative of three independent experiments (n = 6). Data are normalized against control and are expressed as mean ± SEM. ***$P < 0.001$, Mann Whitney test. (C) Representative images of pHrodo-PFFs in primary hippocampal neurons. Data are representative of three independent experiments. Scale bar: 20 μm. (D) (E) (F) Area of pHrodo-dextran in primary hippocampal neurons. In Fig. 3D–3G, “control” refers to the primary neurons that were transduced with pHrodo-dextran and treated with vehicle. Plotted data are representative of three independent experiments (n = 4–6). Data are normalized against control and are expressed as mean ± SEM. **$P < 0.01$, ***$P < 0.001$, Kruskal-Wallis test with Dunn’s *post hoc* test (D), and Mann Whitney test (E, F). (G) Representative images of pHrodo-dextran in primary hippocampal neurons. Data are representative of three independent experiments. Scale bar: 20 μm.

FIG. 4

PER inhibits the development of p-α-syn–positive pathology in a mouse model of PD. (A) Level of total α-syn in the Triton X-soluble fraction. The numbers (in kDa) to the right indicate the position of the size markers. Representative images and plotted data are

shown (n = 5). All values are expressed as mean ± SEM. N.S.: Not significant, Mann Whitney test. (B) Level of p-α-syn in the Triton X-soluble fraction. The numbers (in kDa) to the right indicate the position of the size markers. Representative images and plotted data are shown (n = 5). All values are expressed as mean ± SEM. N.S.: Not significant, Mann Whitney test. (C) Time schedule for the injection of α-syn PFFs and drug treatment. In Fig. 4, “PER (pre)” refers to “the mice in which PER treatment was initiated prior to the injection of α-syn PFFs,” whereas “PER (post)” refers to “the mice in which PER treatment was initiated after the injection of α-syn PFFs.” (D) Representative images of immunohistochemical staining of the mice that underwent injection of α-syn PFFs and drug treatment. Insets show high-power images of p-α-syn-positive pathology in the AON and PC. Data are representative of two independent experiments. Scale bar: 200 μm; inset: 50 μm. (E) Area of p-α-syn-positive pathology in the AON and PC. Plotted data are pooled from two independent experiments (n = 6–8). Data are normalized against control and are expressed as mean ± SEM. *$P < 0.05$, **$P < 0.01$, N.S.: Not significant, Kruskal-Wallis test with Dunn’s *post hoc* test. (F) Numbers of neuronal p-α-syn-positive aggregates in the AON and PC. Plotted data are pooled from two independent experiments (n = 6–8). Data are normalized against control and are expressed as mean ± SEM. **$P < 0.01$, N.S.: Not

588 significant, Kruskal-Wallis test with Dunn's *post hoc* test. (G) Level of p-α-syn in the Triton
589 X-insoluble fraction. The numbers (in kDa) to the right indicate the position of the size
590 markers. Representative images and plotted data are shown (n = 5). All values are
591 expressed as mean ± SEM. *$P < 0.05$, Kruskal-Wallis test with Dunn's *post hoc* test.
592
593 **Supporting Information FIG. S1**
594 Most of the cells colocalized with pHrodo-PFFs are NeuN-positive cells. (A) Numbers of
595 NeuN or GFAP-positive cells per field. Plotted data are representative of three
596 independent experiments (n = 8). Data are expressed as mean ± SEM. (B) Numbers of
597 NeuN or GFAP-positive cells per field colocalized with pHrodo-PFFs. Plotted data are
598 representative of three independent experiments (n = 8). Data are expressed as mean ±
599 SEM.
600
601 **Supporting Information FIG. S2**
602 NBQX and TTX show no toxicity to primary neuronal culture. (A) (B) Density of neurons.
603 Data are representative of three independent experiments (n = 6). Data are normalized
604 against control and are expressed as mean ± SEM. N.S.: Not significant, Mann Whitney

test. Scatter plots show data from each sample. (C) (D) LDH assay. Plotted data are representative of three independent experiments (n = 6). Data are normalized against control and are expressed as mean ± SEM. N.S.: Not significant, Mann Whitney test.

622 Financial disclosure of all authors (for the preceding 12 months)

623 J.U. and T.T. have no financial disclosure. N.U. received Japan Society for the
624 Promotion of Science (JSPS) Overseas Research Fellowships. M.S. received grants from
625 JSPS and Sumitomo Dainippon Pharma Co., Ltd. M.I. received a grant from JSPS. S.K.
626 received a grant from JSPS. Y.T. is a principal investigator of clinical trials by Kyowa Kirin
627 Co., Ltd., and Kissei Pharmaceutical Co., Ltd., and received a grant from JSPS. S.M.
628 received grants from JSR Co., Ltd, ROHTO Pharmaceutical Co., Ltd, and NOASTEC
629 Foundation. H.Y. received grants from JSPS. R.T. received consultancies from KAN
630 Research Institute, Inc., Ono Pharmaceutical Co., Ltd., Chugai Pharmaceutical Co., Ltd.;
631 grants/research support from Sumitomo Dainippon Pharma Co., Ltd., Takeda
632 Pharmaceutical Co., Ltd., Eisai Co., Ltd., Kyowa Kirin Co., Ltd., Sanofi K.K., Otsuka
633 Pharmaceutical Co., Ltd., and Nippon Boehringer Ingelheim Co., Ltd.; grants from Japan
634 Agency for Medical Research and Development (AMED), JSPS, and Ministry of Education
635 Culture, Sports, Science and Technology Japan; and honoraria from Sumitomo Dainippon
636 Pharma Co., Ltd., Takeda Pharmaceutical Co., Ltd., Novartis Pharma K.K., Kyowa Kirin
637 Co., Ltd., Eisai Co., Ltd., Otsuka Pharmaceutical Co., Ltd., Ono Pharmaceutical Co., Ltd.,
638 AbbVie Inc, and Alexion Pharmaceuticals, Inc.

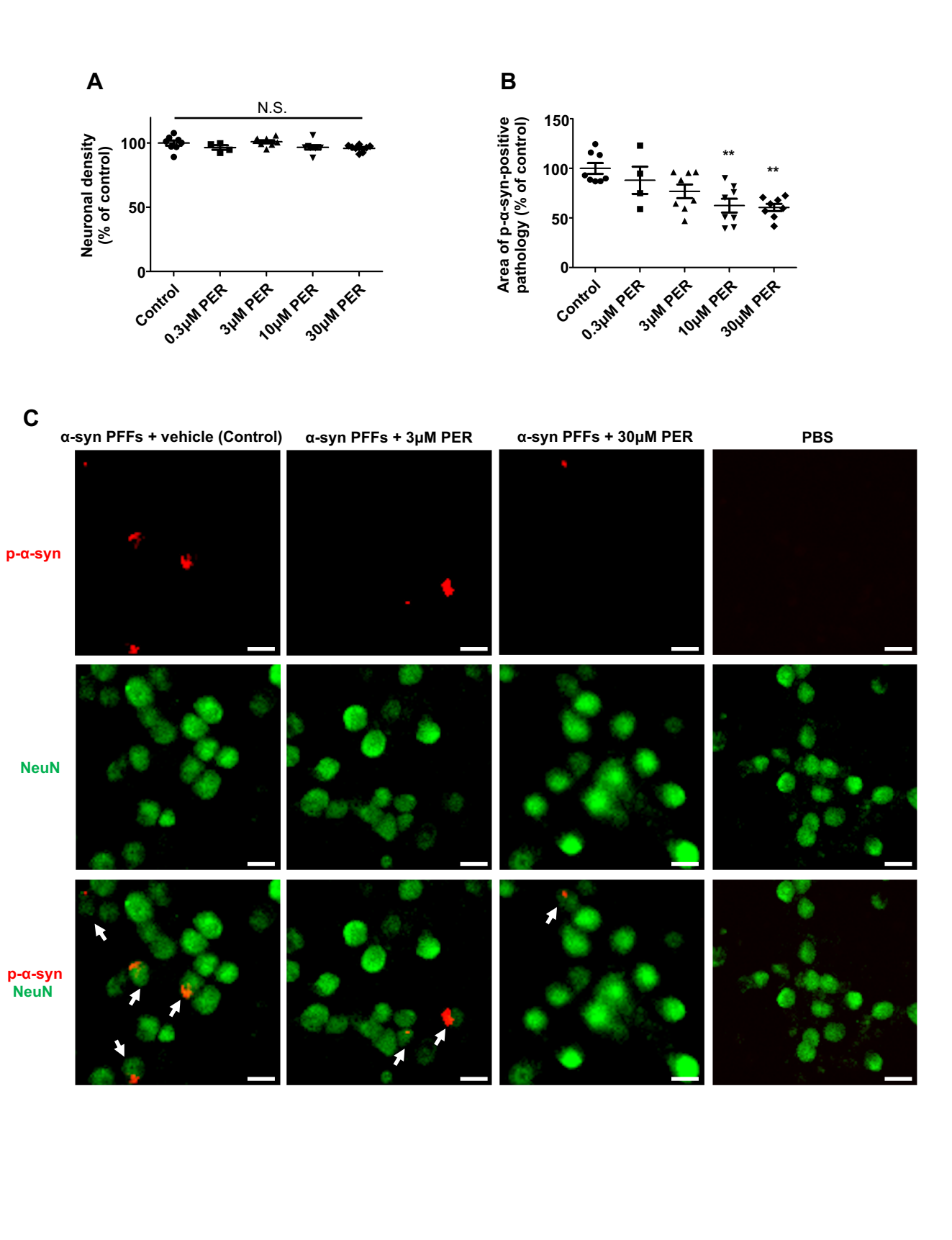
A
N.S.
Neuronal density (% of control)
100
50
0
Control
0.3μM PER
3μM PER
10μM PER
30μM PER
B
Area of p-α-syn-positive pathology (% of control)
150
100
50
0
**
**
Control
0.3μM PER
3μM PER
10μM PER
30μM PER
C
α-syn PFFs + vehicle (Control)
α-syn PFFs + 3μM PER
α-syn PFFs + 30μM PER
PBS
p-α-syn
NeuN
p-α-syn
NeuN

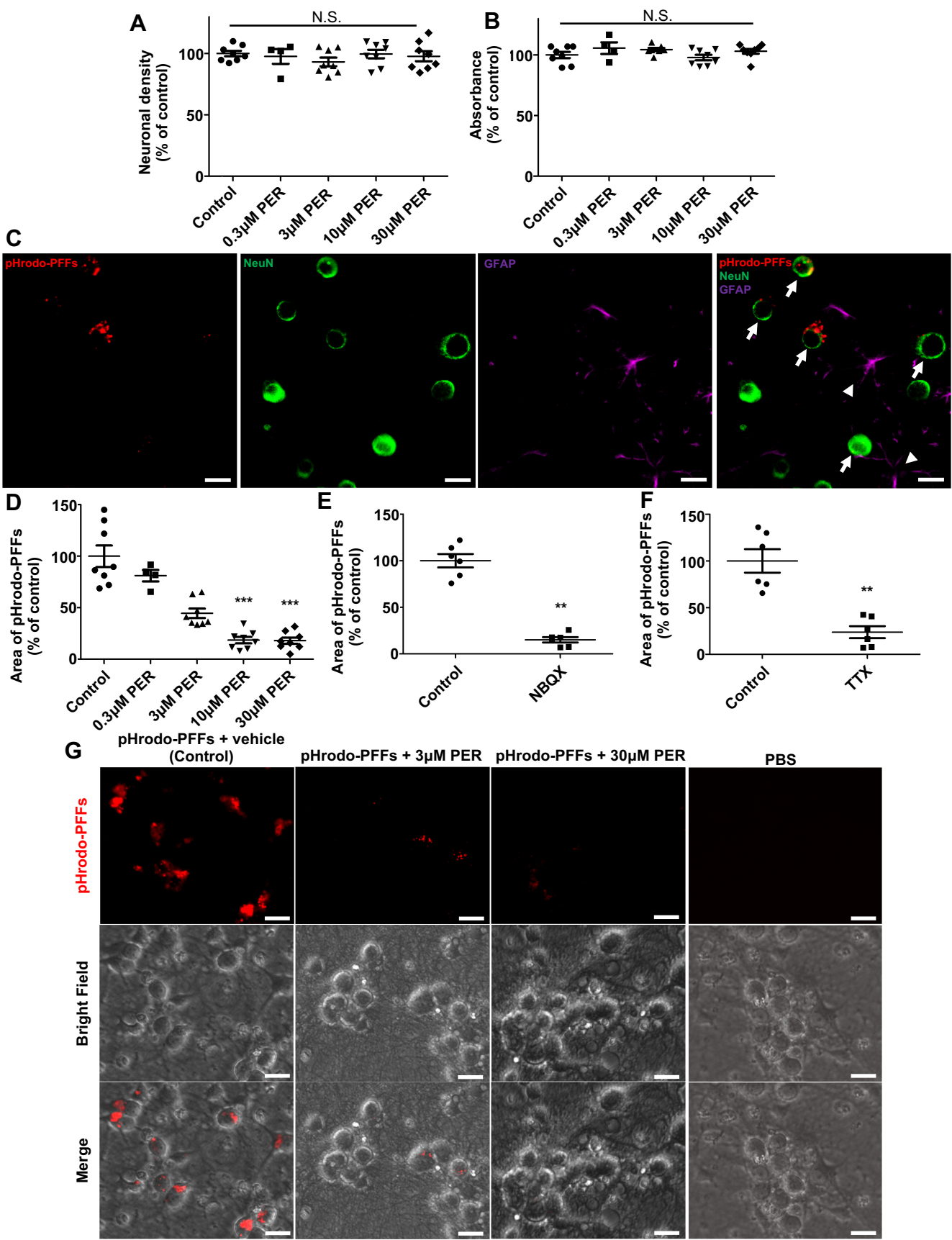
A
N.S.
Neuronal density (% of control)
100
50
0
Control
0.3μM PER
3μM PER
10μM PER
30μM PER
B
N.S.
Absorbance (% of control)
100
50
0
Control
0.3μM PER
3μM PER
10μM PER
30μM PER
C
pHrodo-PFFs
NeuN
GFAP
pHrodo-PFFs
NeuN
GFAP
D
Area of pHrodo-PFFs (% of control)
150
100
50
0
***
***
Control
0.3μM PER
3μM PER
10μM PER
30μM PER
E
Area of pHrodo-PFFs (% of control)
150
100
50
0
**
Control
NBQX
F
Area of pHrodo-PFFs (% of control)
150
100
50
0
**
Control
TTX
G
pHrodo-PFFs + vehicle (Control)
pHrodo-PFFs + 3μM PER
pHrodo-PFFs + 30μM PER
PBS
pHrodo-PFFs
Bright Field
Merge

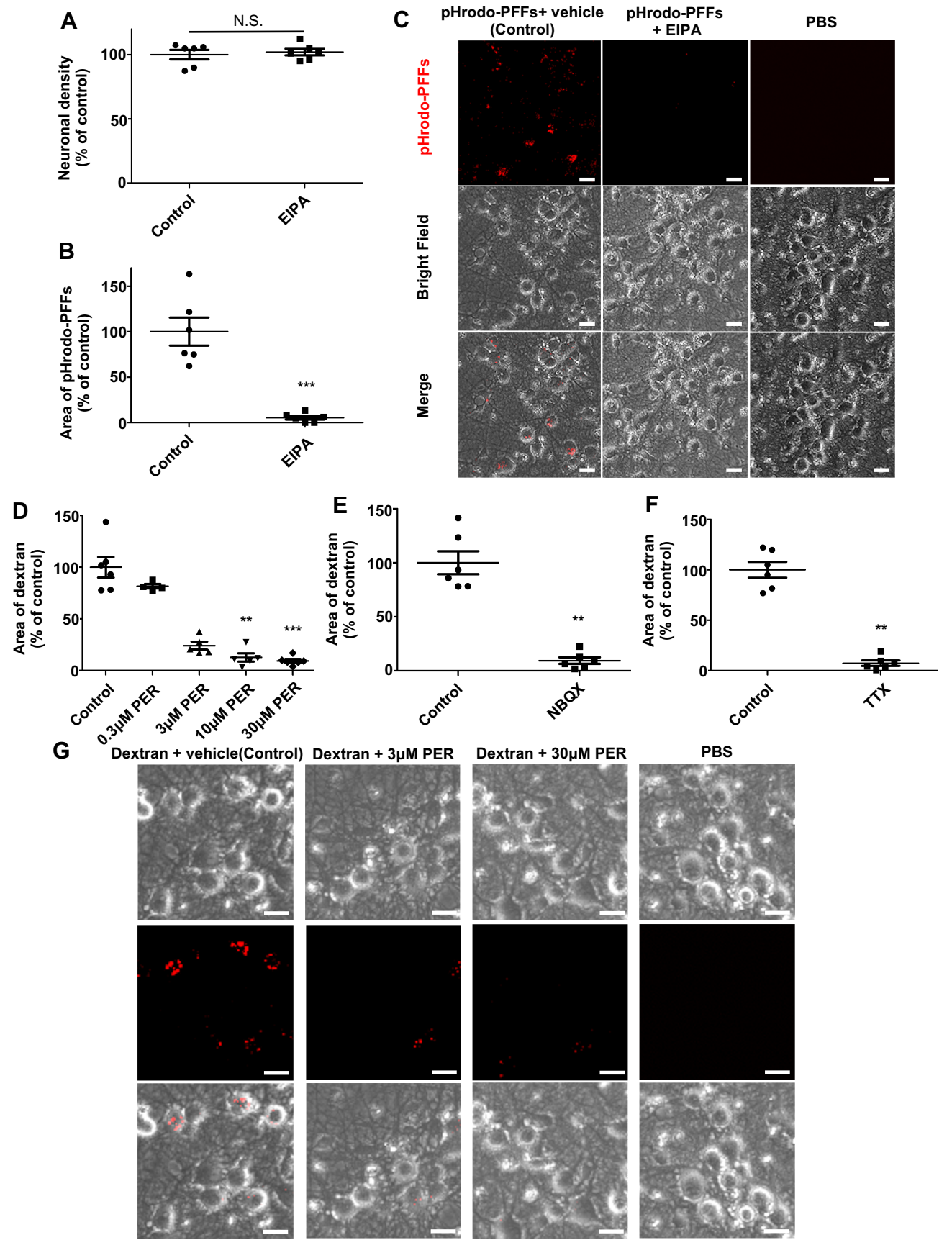
A
N.S.
Neuronal density (% of control)
100
50
0
Control
EIPA
B
Area of pHrodo-PFFs (% of control)
150
100
50
0
***
Control
EIPA
C
pHrodo-PFFs+ vehicle (Control)
pHrodo-PFFs + EIPA
PBS
pHrodo-PFFs
Bright Field
Merge
D
Area of dextran (% of control)
150
100
50
0
**
***
Control
0.3μM PER
3μM PER
10μM PER
30μM PER
E
Area of dextran (% of control)
150
100
50
0
**
Control
NBQX
F
Area of dextran (% of control)
150
100
50
0
**
Control
TTX
G
Dextran + vehicle(Control)
Dextran + 3μM PER
Dextran + 30μM PER
PBS

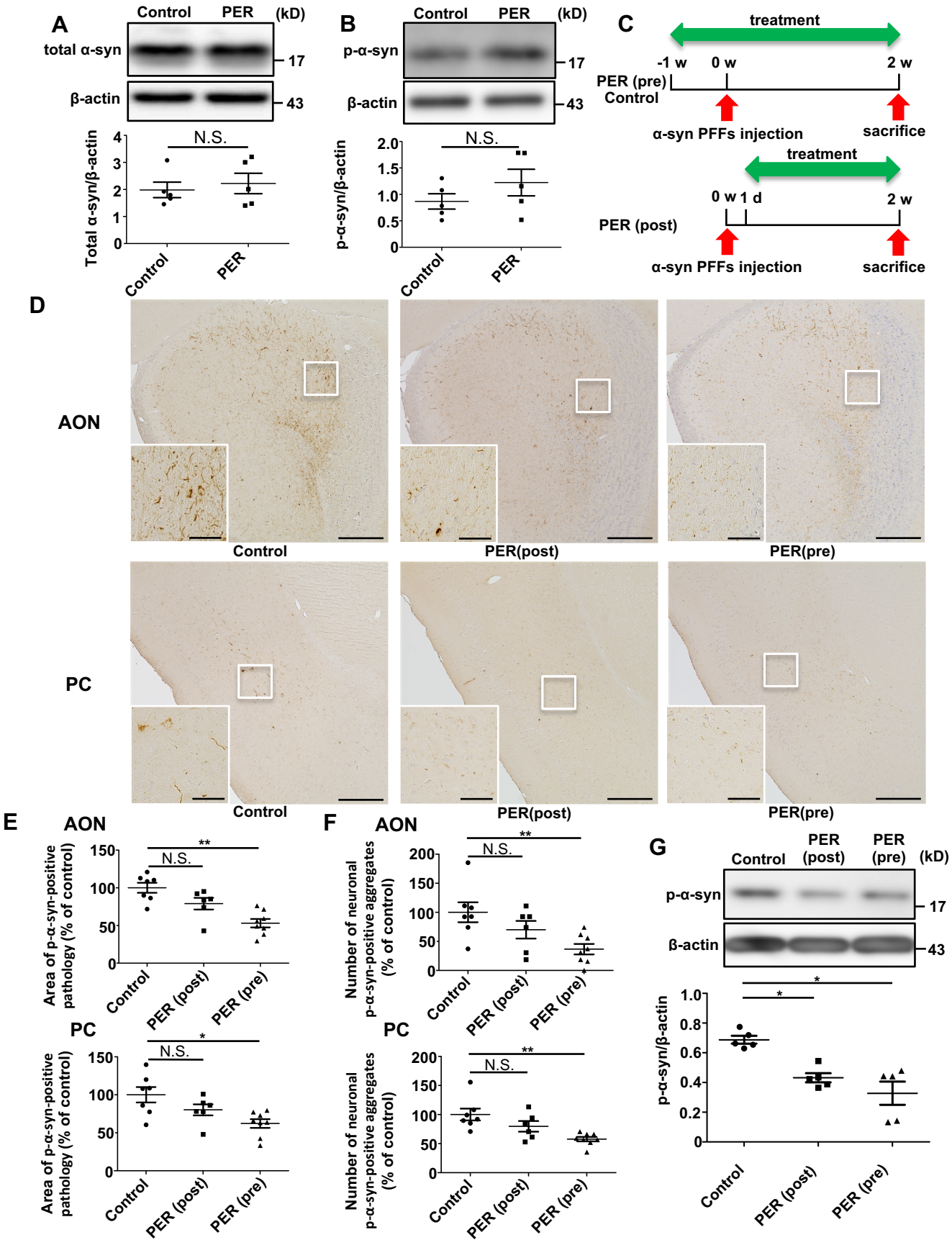
A
Control
PER
(kD)
total α-syn
17
β-actin
43
Total α-syn/β-actin
N.S.
Control
PER
B
Control
PER
(kD)
p-α-syn
17
β-actin
43
p-α-syn/β-actin
N.S.
Control
PER
C
treatment
-1 w
0 w
2 w
PER (pre)
Control
α-syn PFFs injection
sacrifice
treatment
0 w
1 d
2 w
PER (post)
α-syn PFFs injection
sacrifice
D
AON
PC
Control
PER(post)
PER(pre)
Control
PER(post)
PER(pre)
E
AON
Area of p-α-syn-positive pathology (% of control)
N.S.
**
Control
PER (post)
PER (pre)
PC
Area of p-α-syn-positive pathology (% of control)
N.S.
*
Control
PER (post)
PER (pre)
F
AON
Number of neuronal p-α-syn-positive aggregates (% of control)
N.S.
**
Control
PER (post)
PER (pre)
PC
Number of neuronal p-α-syn-positive aggregates (% of control)
N.S.
**
Control
PER (post)
PER (pre)
G
Control
PER (post)
PER (pre)
(kD)
p-α-syn
17
ß-actin
43
p-α-syn/β-actin
*
*
Control
PER (post)
PER (pre)

Fig.S1

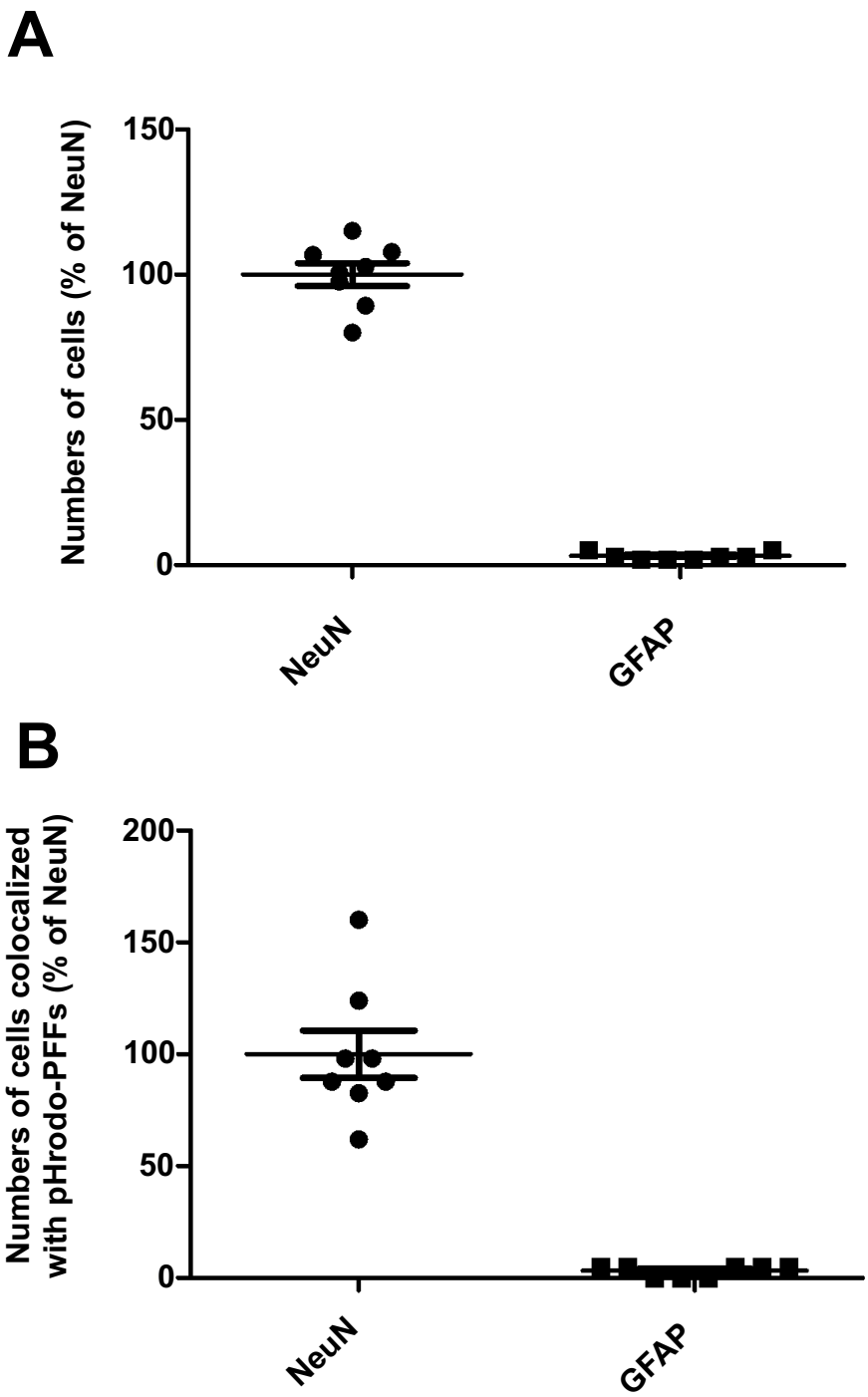
A
Numbers of cells (% of NeuN)
150
100
50
0
NeuN
GFAP
B
Numbers of cells colocalized with pHrodo-PFFs (% of NeuN)
200
150
100
50
0
NeuN
GFAP

Fig.S2

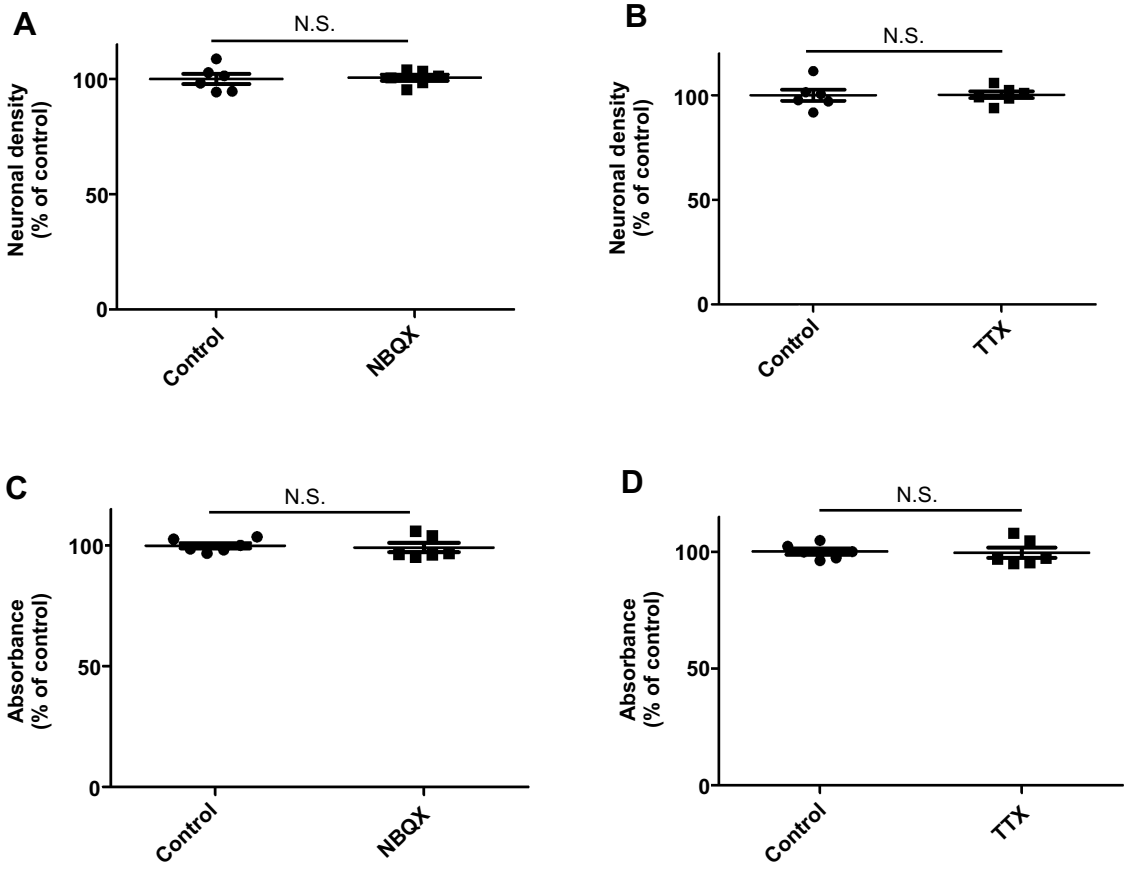
A
N.S.
Neuronal density
(% of control)
100
50
0
Control
NBQX
B
N.S.
Neuronal density
(% of control)
100
50
0
Control
TTX
C
N.S.
Absorbance
(% of control)
100
50
0
Control
NBQX
D
N.S.
Absorbance
(% of control)
100
50
0
Control
TTX